

Differential Mechanisms of Activation of the Ang Peptide Receptors AT1, AT2, and MAS: Using *In Silico* Techniques to Differentiate the Three Receptors

Jeremy W. Prokop¹, Robson A. S. Santos², Amy Milsted^{1*}

¹ Department of Biology, Program in Integrated Bioscience, The University of Akron, Akron, Ohio, United States of America, ² Departamento de Fisiologia e Biofísica, Instituto de Ciências Biológicas, Federal University of Minas Gerais, Belo Horizonte, Minas Gerais, Brazil

Abstract

The renin-angiotensin system is involved in multiple conditions ranging from cardiovascular disorders to cancer. Components of the pathway, including ACE, renin and angiotensin receptors are targets for disease treatment. This study addresses three receptors of the pathway: AT1, AT2, and MAS and how the receptors are similar and differ in activation by angiotensin peptides. Combining biochemical and amino acid variation data with multiple species sequence alignments, structural models, and docking site predictions allows for visualization of how angiotensin peptides may bind and activate the receptors; allowing identification of conserved and variant mechanisms in the receptors. MAS differs from AT1 favoring Ang-(1–7) and not Ang II binding, while AT2 recently has been suggested to preferentially bind Ang III. A new model of Ang peptide binding to AT1 and AT2 is proposed that correlates data from site directed mutagenesis and photolabeled experiments that were previously considered conflicting. Ang II binds AT1 and AT2 through a conserved initial binding mode involving amino acids 111 (consensus 325) of AT1 (Asn) interacting with Tyr (4) of Ang II and 199 and 256 (consensus 512 and 621, a Lys and His respectively) interacting with Phe (8) of Ang II. In MAS these sites are not conserved, leading to differential binding and activation by Ang-(1–7). In both AT1 and AT2, the Ang II peptide may internalize through Phe (8) of Ang II propagating through the receptors' conserved aromatic amino acids to the final photolabeled positioning relative to either AT1 (amino acid 294, Asn, consensus 725) or AT2 (138, Leu, consensus 336). Understanding receptor activation provides valuable information for drug design and identification of other receptors that can potentially bind Ang peptides.

Citation: Prokop JW, Santos RAS, Milsted A (2013) Differential Mechanisms of Activation of the Ang Peptide Receptors AT1, AT2, and MAS: Using *In Silico* Techniques to Differentiate the Three Receptors. PLoS ONE 8(6): e65307. doi:10.1371/journal.pone.0065307

Editor: Michael Bader, Max-Delbrück Center for Molecular Medicine (MDC), Germany

Received: March 27, 2013; **Accepted:** April 25, 2013; **Published:** June 3, 2013

Copyright: © 2013 Prokop et al. This is an open-access article distributed under the terms of the Creative Commons Attribution License, which permits unrestricted use, distribution, and reproduction in any medium, provided the original author and source are credited.

Funding: Funding was through Choose Ohio First Bioinformatics scholarship, University of Akron, American Heart Association award 11PRE7380033, Brazilian National Institute of Science and Technology in Hormones and Women's Health, and Federal University of Minas Gerais. The funders had no role in study design, data collection and analysis, decision to publish, or preparation of the manuscript.

Competing Interests: The authors have declared that no competing interests exist.

* E-mail: milsted@uakron.edu

Introduction

The renin-angiotensin system (RAS) is a critical homeostatic pathway controlling blood volume and pressure. The pathway is central to homeostasis of blood pressure, and perturbation of steps in this pathway is associated with disease phenotypes, including hypertension, cardiac hypertrophy and fibrosis (reviewed in [1]). In addition, products or components of the RAS influence many other physiological systems such as brain development and reproduction, which is why understanding the details of how the RAS functions is of high importance. Structures of many components of the RAS are known (Table 1) or can be modeled, allowing for a protein structural diagram of the RAS (Figure 1). The RAS begins with the expression of angiotensinogen (AGT), which can exist in either a reduced or oxidized state [2]. The enzyme renin is expressed in a non-enzymatic pro-form [3], activated through either binding to the (pro)renin receptor [4] or enzymatic cleavage of the pro-domain. When activated, renin cleaves a ten amino acid peptide from AGT known as Ang I. This peptide is cleaved in various ways resulting in numerous peptides. The most well defined of these peptides is the cleavage of amino acids nine and ten from Ang I resulting in Ang II by enzymes such

as ACE. This peptide is then further processed by enzymes such as ACE 2 to yield Ang-(1–7) [5] or by aminopeptidases to yield Ang III (amino acids 2–8 of Ang II) [6]. Having protein structures of each one of these steps allows for critical understanding of details in how each step works, allowing for novel drug design targeted to the critical steps of the pathway.

The Ang peptides with the most potent effect on the cardiovascular system are Ang II and Ang-(1–7). Ang II is the most studied, with known interactions with AT1 [7] and AT2 [8] receptors. Ang II binds to AT1 eliciting a blood pressure increase [9]/proangiogenic/proliferative effect [10], or to AT2, yielding a blood pressure decrease [11]/antiangiogenic/antiproliferative effect [12] effect. Gene knockout studies of AT2 show increased blood pressure [11], yet animal research with agonists of AT2 has not shown significant lowering of blood pressure, suggesting that AT2 probably serves more of a role in vascular remodeling or inhibition of AT1 (reviewed in [8]). AT1 and AT2 are members of a large family of G-protein coupled receptors (GPCRs), all sharing seven transmembrane helices. Ang-(1–7) has been shown to activate the proto-oncogene MAS product, stimulating similar pathways as AT2 activated by Ang II [13,14]. Several highly homologous MAS-related genes have also been suggested to be

Table 1. Known structures of the renin-angiotensin system.

Protein	pdb ID	Information	Species
(Pro)renin	3vcm	Human Prorenin	Human
Renin	1bbs	Native	Human
Renin	2ren	Native	Human
Renin	2v0z	Aliskiren bound	Human
(Pro)renin receptor	3lbs	(pro)renin Receptor MBP fusion	Human
Agt	2wxw	Oxidized	Human
Agt	2wxx	Oxidized	Mouse
Agt	2wxy	Reduced	Mouse
Renin-Agt	2x0b	Complexed together	Human
Ang I	1n9u	Solution structure	Multiple
ACE N-term	2c6f	Native	Human
ACE N-term	2c6n	Lisinopril bound	Human
ACE C-term	1o8a	Native	Human
ACE C-term	1o86	Lisinopril bound	Human
Ang II	1n9v	Solution structure	Multiple
ACE2	1r42	Native	Human
ACE2	1r4l	MLN-4760 bound	Human
Ang-(1-7)	2jp8	Solution structure	Multiple

doi:10.1371/journal.pone.0065307.t001

activated by Ang peptides [15]. Like AT1 and AT2, MAS and its related proteins are GPCRs, all of which fall into class A or Rhodopsin-like GPCRs. As of now, we do not have structures for AT1, AT2, or MAS receptors. The structure of rhodopsin has been used in many studies modeling AT1 [16–19] and AT2 [20], but less work has been done on modeling MAS. Using these models, it may be possible to determine how the Ang peptides bind to each receptor and how binding alters the structure to active intracellular pathways. GPCRs readily form homo- or heterodimers with other proteins [21,22], and this likely functions into the intracellular activation of the pathway. Using protein modeling techniques, sequence alignments, molecular dynamics, docking

predictions of Ang peptides and known functional data of AT1, AT2, and MAS, it is possible to address both the role of any conserved binding regions for the Ang peptides in these receptors and potential protein-protein interactions with other membrane proteins.

Materials and Methods

Generation of Models for AT1, AT2 and MAS

Figure 2A shows the methods used to model each receptor. Models for human AT1 [Uniprot: P30556], AT2 [Uniprot: P50052] and MAS [Uniprot: P04201] were created with I-TASSER [23,24]. Disulfide bonds were added to AT1 and AT2 and energy minimized with AMBER03 [25] force field in 0.997 g/mL of water. The structure of AT1 was then placed into a lipid membrane of phosphatidylethanolamine and simulation run with the standard md_runmembrane macro (<http://www.yasara.org/macros.htm>) on YASARA. Simulations were run for 2000 picoseconds (ps) of which the first 250 ps were restrained equilibration simulation. The average structure throughout the simulation was used as the model for AT1. The AT2 and MAS models were independently aligned with the AT1/membrane complex, the AT1 removed and simulations run with the md_runmembrane macro. The average structure for each of these was used as the model for each protein (Figure 2B). Alignments of the protein models were performed with Mustang [26] and compared to the structure of Rhodopsin [PDB: 1 gzm] to show similarity in the family.

Sequence Alignments

Sequences of MAS from multiple species included human [Uniprot: P04201], mouse [Uniprot: P30554], rat [P12526], common chimpanzee [Predicted Gene ID: 472176], macaque (Predicted Gene ID: 703105), naked mole rat [Uniprot: G5BC59], dog [Predicted Gene ID: 484066], and Chinese hamster [Uniprot: G3HGQ0] were aligned using ClustalW. The same was done for AT1 sequences from human [Uniprot: P30556], rat [Uniprot: P25095 and P29089], mouse [Uniprot: P29754], rabbit [Uniprot: P34976], pig [Uniprot: P30555], common chimpanzee [Uniprot: Q9GLN9], Mongolian gerbil [Uniprot: O35210], guinea pig [Uniprot: Q9WV26], dog [Uniprot: P43240], sheep [Uniprot:

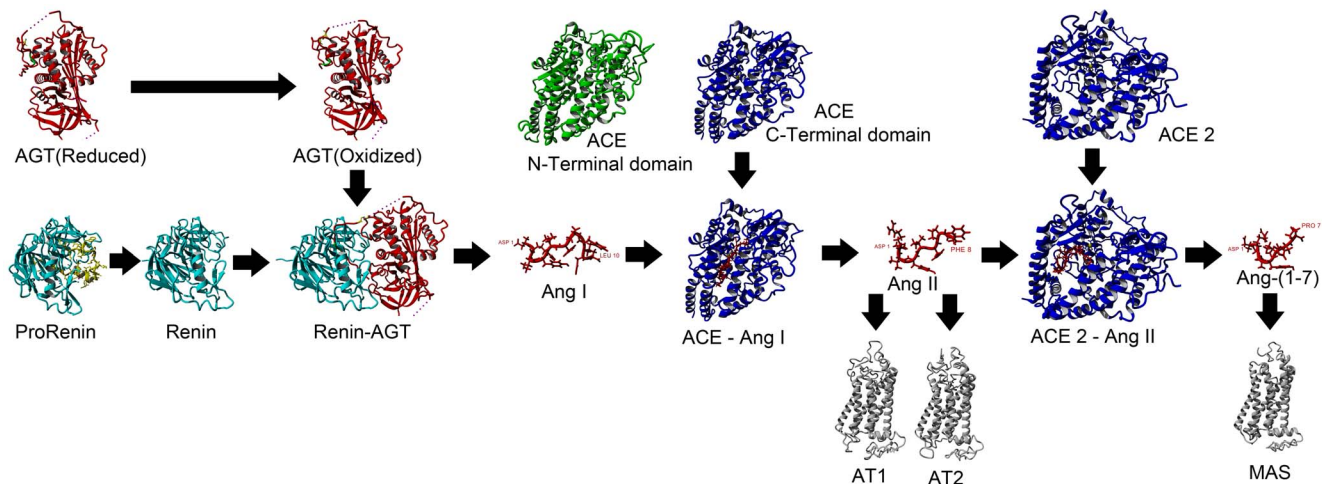


Figure 1. The renin-angiotensin system shown in protein structures based on available or modeled structures. Angiotensinogen (AGT, red) is cleaved by Renin (cyan) producing the ten amino acid Ang I peptide. Ang I is then cleaved by ACE to produce Ang II that is subsequently cleaved by ACE 2 to produce Ang-(1-7). These peptides then bind to AT1, AT2, or MAS (gray).

doi:10.1371/journal.pone.0065307.g001

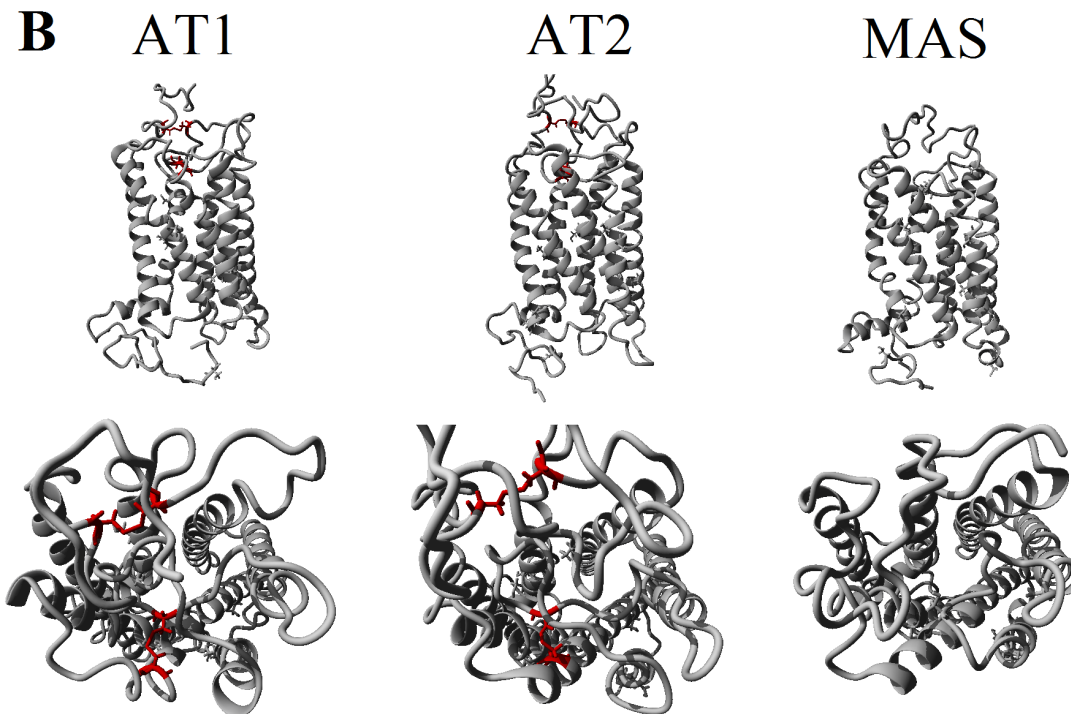
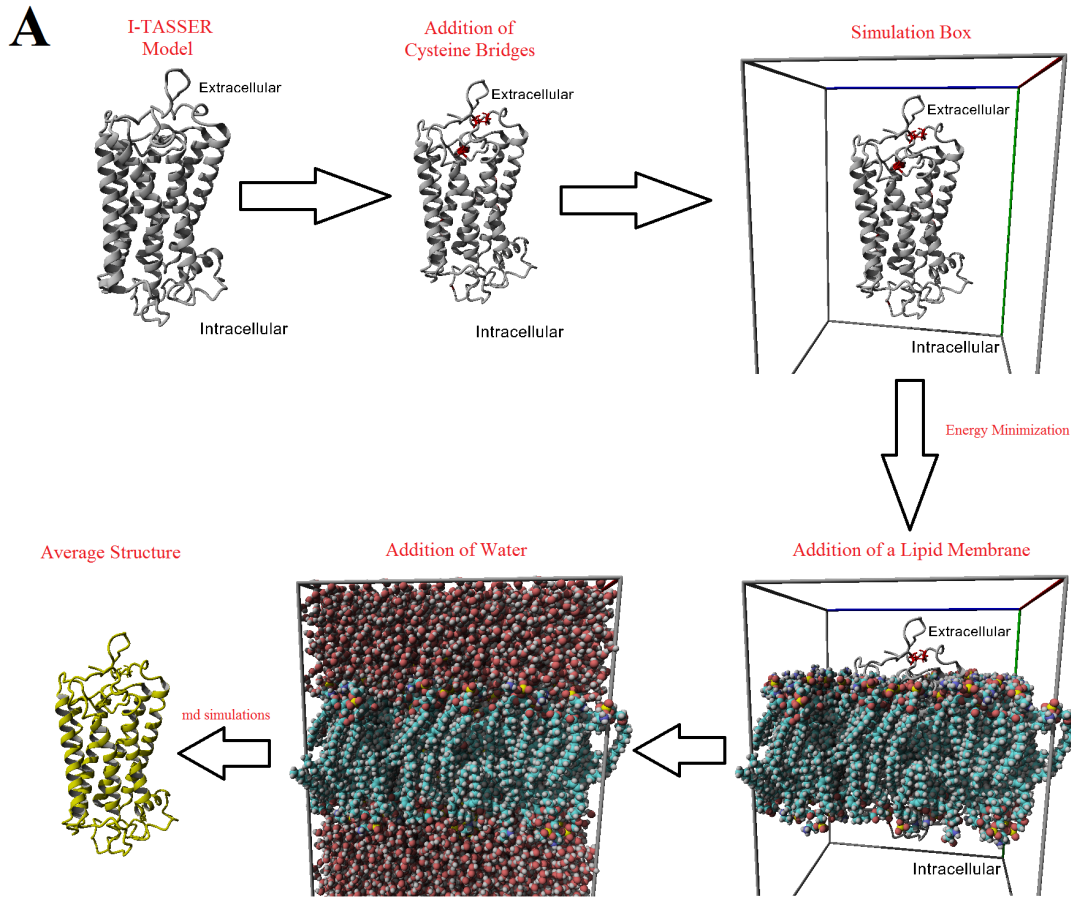


Figure 2. Models for AT1, AT2, and MAS. A) Methodology for creating models of AT1, AT2 and MAS beginning with I-TASSER models, adding cysteine bridges, inserting into a lipid membrane and then running molecular dynamics simulations. B) The averaged models from A for AT1, AT2, and MAS.

doi:10.1371/journal.pone.0065307.g002

O77590, chicken [Uniprot: P79785], cattle [Uniprot: P25104], wild turkey [Uniprot: P33396] and AT2 from human [Uniprot: P50052], mouse [Uniprot: P35374], rat [Uniprot: P35351] and Mongolian gerbil [Uniprot: Q9Z0Z6]. The compiled AT1, AT2, and MAS sequences were aligned with the human sequences of each using ClustalW, and the consensus sequences added into the alignment manually. These sequence alignments were compared to the sequence of human rhodopsin [Uniprot: P08100]. Numbering and identification of conserved GPCR amino acids were based on consensus GPCR numbers with AT1 alignments [18]. The numbering system of GPCRs was used with the hundred place as the helix number followed by the next sequential amino acid (101 is the first amino acid on helix one).

Docking Ang Peptides

To identify the best docking sites in each model, the `dock_runensemble` macro (<http://www.yasara.org/macros.htm>) was used with default twenty docking experiments of the ligand on six possible ensembles of the receptor for AT1 or MAS with Ang II or Ang-(1–7). The simulation square was 30 Å on the x, y, and z axis and placed in the proposed binding site. As the initial model had problems with the extracellular domains filling the active site, the region between helix 4 and 5 was deleted to open up the active site. The top ten docking results of each independent run were then treated with the `docking_EM_analysis` macro (`Docking_EM_analysis S1`) calculating the potential energy of the receptor, potential energy of the ligand, binding energy of the ligand and movement of the energy minimized structures from the initial structure. For each receptor/ligand data set (containing ten complexes) rankings for the highest value for each binding energy of the ten members of the experiment were made and the scores compiled with the three lowest values selected for further treatment.

The top three of each energy minimized receptor/ligand complex were then analyzed by showing the amino acids conserved among AT1, AT2, and MAS or by binding the ligand to the other receptors with the `Docking_EM_top3` macro (`Docking_EM_top3 S1`). In short, each of the three possible ligand confirmations of the complexes were energy minimized to AT1, AT2, MAS, or Rhodopsin and the potential energy of the receptor and the binding energy of the ligand was calculated. A forced docking experiment (known as initial docking) was also conducted using the known biochemical data of amino acids 512 (Lys) and 621 (His). To create this model the first of the multiple Ang II peptide models as determined by NMR [27] was manually placed so that the C-terminus of Ang II is interacting with amino acid 512 [28,29] (Lys) and amino acid 8 (Phe) of Ang II interacting with 621 (His) [30]. Twenty manual dockings (all of which had slightly different orientations of amino acid 8) were performed using energy minimizations of the AT1 model in a lipid membrane, and binding energies were calculated to determine the top three forced dockings. These top three were then run through the `Docking_EM_top3` macro and compared to the top binding energy of the docking experiments above. Alternatively, a second set of twenty forced dockings (known as buried docking) were performed using the known photolabeled data which places the C-terminus close to consensus amino acid 725 (Asn) [31]. These dockings were analyzed in the same manner as the initial docking.

The multiple states of docking were aligned into the structure of AT1 in the lipid membrane using MUSTANG algorithm [26], energy minimized with AMBER03 force field in water, and molecular dynamics performed for 10 nanoseconds.

Results

The Ang peptide receptors AT1, AT2, and MAS are not yet present in the protein data bank (PDB). These structures were modeled (Figure 2A), using a lipid membrane and molecular dynamics simulations to determine the average structure for each (Figure 2B). For all models the structure of Rhodopsin showed low levels of sequence homology (with 14–21% homology) with structures that showed higher homologies (Table 2). The models were threaded primarily using the structure of NK1R [pdb: 2ks9] in I-TASSER, a program highly validated in modeling of GPCRs [32]. Molecular dynamics simulations in the lipid membrane resulted in models of AT1, AT2, and MAS that had similar energies (Figure 3A) and carbon alpha RMSDs (Figure 3B). It should be noted that MAS could potentially contain a Cys bridge, but this bridge was left out of simulations in Figure 3 as it does not significantly alter the energy and movement of the models (Figure S1). Looking at the averaged movement of each amino acid over the entire simulation shows that the seven transmembrane domains are all stabilized in AT1, AT2, and MAS with much higher RMSD in all loops (Figure S2).

Consensus sequence alignments were used to compare MAS, AT1, and AT2 from multiple species which were then compared to Rhodopsin. AT1 sequences were identified from fourteen species (Figure S3), AT2 from four species (Figure S4), and MAS from eight species (Figure S5). Aligning the human and the consensus sequences from AT1, AT2, and MAS with human Rhodopsin sequences allows for the identification of common GPCR conserved amino acids (Figure 4, red), those conserved in all (Figure 4, cyan), those only conserved in AT1, AT2, and MAS but not Rhodopsin (Figure 4, green) and those conserved in only AT1 and AT2 (Figure 4, gray and magenta). We next identified known natural variants associated with disease as well as mutational data suggesting amino acids of importance (Table S1). The locations of these amino acids were then identified on the sequence alignments (Figure 4, bold and underlined) and conservation in all sequences determined. Of all the natural variants known, only amino acid 517, present as a Phe, is conserved in all three receptors; this is also conserved in Rhodopsin and many other GPCRs. The Table S1 reveals several potentially functional amino acids at 224 (Asp), 336 (Leu), 725 (Asn) and 729 (Asn) that are conserved in all three receptors. Of these only 725 (Asn) is not conserved in Rhodopsin and thus represents a possible target for specific interaction with Ang peptides conserved in AT1, AT2 and MAS.

Combining a structural model of AT1 with the functionally conserved amino acids seen in sequence alignments (using the same coloring for identification of conservation) reveals that amino acid 725 (Asn) is found in the binding pocket of all three receptors (Figure 5). Amino acids 118, 231, 233, 268, 334, 337, 508, 622, and 719 are conserved in the binding pockets of AT1, AT2 and MAS but are not conserved in Rhodopsin (Figure 5, green), all suggesting potential interactions with Ang peptides. Only amino

Table 2. Sequence and structural alignment values of AT1, AT2, MAS, and Rhodopsin.

	Rhodopsin	AT1	AT2	MAS	
Rhodopsin	–	19.53%	21.79%	14.51%	
AT1	1.862 Å	–	37.80%	20.25%	% Sequence Homology
AT2	1.963 Å	2.05 Å	–	20%	
MAS	2.081 Å	1.938 Å	1.984 Å	–	
	RMSD of models				

doi:10.1371/journal.pone.0065307.t002

acid 622 (Gln) is currently known to have a functional role in Ang II binding (Table S1). Amino acids in the structure of AT1 (Figure 5) with the amino acid and numbers added, are those that

have been identified to contribute to either Ang peptide binding or activation based on previous bench top experiments.

The first very interesting amino acid to have functional importance shown is an Asn at amino acid 325 (Figure 5,

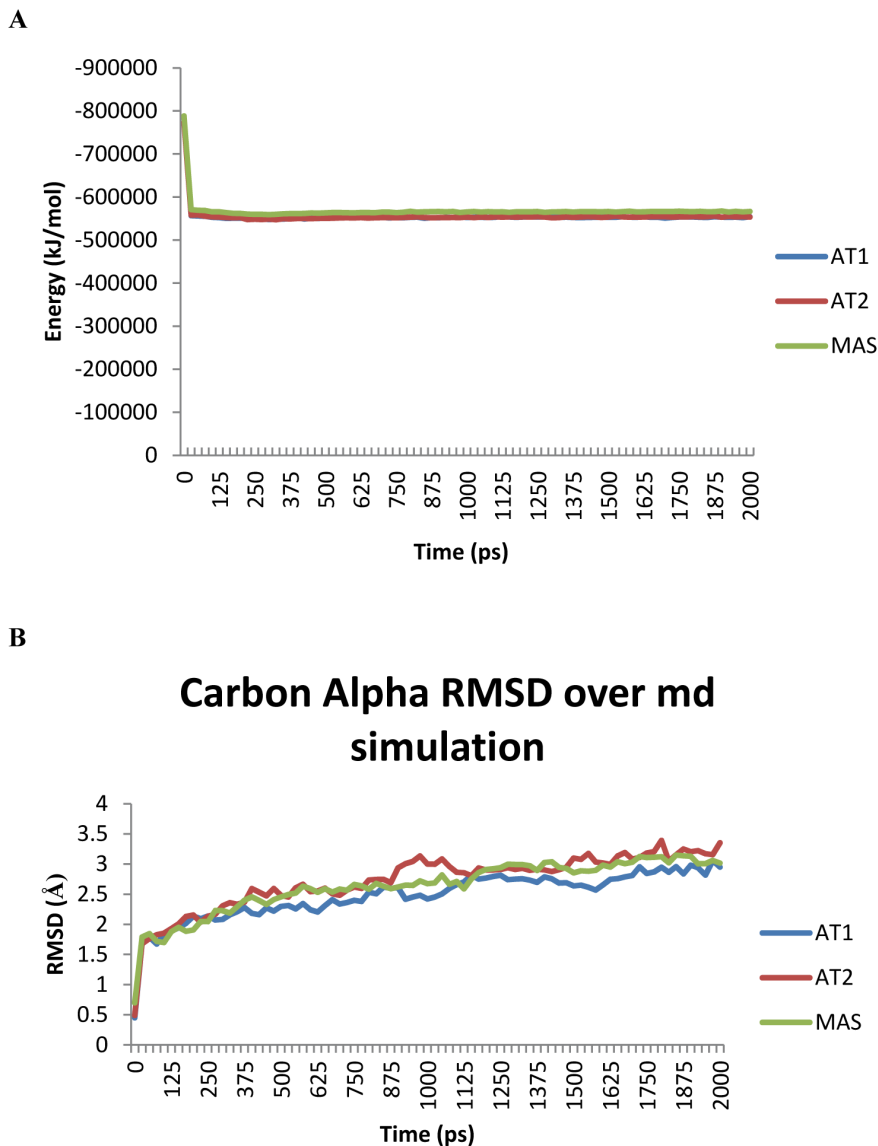


Figure 3. Molecular dynamics of AT1, AT2, and MAS. Simulations of each receptor (AT1, AT2, or MAS) were done in a lipid membrane for 2 nanoseconds showing either the potential energy of the receptor (A) or the averaged carbon alpha root-mean squared deviation (RMSD = average movement of the protein backbone at each amino acid from the initial structure (B)).

doi:10.1371/journal.pone.0065307.g003

AT1_Human	MILNSSTEDGKRIQD-----DCPKAGRHN YIFVMIPTYSIIIFVVGI	43
AT1_Consensus	M.αN.S.ββ.αKRI..-----DCP..GRH. YInαMαPTαYSIIFααGα	
AT2_Human	MKGNSTLATTSKNIITSGLHFGLVNIISGNNESTLNC SQK-PSD KHLDAIPIIYYIIFVIGF	59
AT2_Consensus	MK.N.∞αA.TSμNITS...F..αNα∞G.Nβ..αNCS.K-P.D KHLβAIPαLYαIFVIGF	
MAS_Human	MDGSNVTSFVVEEPTNIS-----TGRNASVGNH RQIPIVHWVIMSISPVG	47
MAS_Consensus	MD..NαT..α.....N.S-----∞.RN.SαG... ..αPαVHWVIMSISPαGF	
Rhodopsin_HUMAN	MNGTEGPNFYVPPFSNATG-----VVRSPFEYPQYLAEP WQFSMLAAYMFLILIVLGF	52

	HELIX 1	HELIX 2	
	130 133 137	214-216 220 224 231 233	268 270 311
AT1_Human	FGNSLVIVV YFYMKLKT VASVFLNLALADLCFLTPT WAVYVTAME YRNPFG NYLCKI		103
AT1_Consensus	FGNSLαVIVI Y.YMKLKT VASαFLNLALADαCFLαTLPαWααYTAME Y.RPFG N.LCKα		
AT2_Human	LVNIVVVTLF CCQKGPKK VSSIIYFNLAVALDLLLATLPLWATYYSYR YDNLFG PVMCKV		119
AT2_Consensus	αVNIαVV∞LF CCQKGPKK VSSIIYFNLAαADL LLLATLPLWATYYSYR YDNLFG PVMCKV		
MAS_Human	VENGILLWFL CFRMR-RN PFTVYITHSIADISLLFCIFILSIDYALD VELSSG HYYTIV		106
MAS_Consensus	VENGILLWFL CF.MR-RN PFTVYITHSIADISLLFCIFILSαDYALD VELSSG ppYTIV		
Rhodopsin_HUMAN	PINFLTLYVT VQHKKLT PLNYIILLNLAVADLFMVLGGFTSLYTSLSH GYVFG PTGCNL		112

	HELIX 3	HELIX 4	
	328 332 337 340 343 347	419 420 425	
AT1_Human	AS-ASVSPNLYASVFLCLSIDRYLAI VHPMKSRLRRTMLV AKVTCIITVLLAGLASLP		162
AT1_Consensus	AS-.αSFLNYASVFLCLSIDRYαAI VHPαKS.IRRTMαα ApVTCααIWLαGαASLP		
AT2_Human	FG-SFLTLMFASIFFIICMSVDRYQSV IYPFLS-QRRNPWQ ASYIVPLVCMACLSLP		177
AT2_Consensus	FG-SFLTLMFASIFFIICMSVDRYQSV IYPFLS-QRRNPWQ ASYαVPLVCMACLSLP		
MAS_Human	TLSVTFLFGYNTGLYLLTAISVERCLSV LYPIWYRCHRPKYQ SALVCALLWALSCLVTTM		165
MAS_Consensus	TLSVTFLFGYNTGLYLLTAISVERCLSV LPIWYRCHRPKπQ SAαVCALLWALSCLαTTM		
Rhodopsin_HUMAN	EG-FFATLGGEIALWLSLVLAIEERYVVV CKEMSN-FRFGENH AIMGVAFTVVMALACAAP		170

	HELIX 5	
	470 508 514 518 520 528	
AT1_Human	AI IHRNVFFIENTNITVCAFHYESQ-NSTLP IGLTKNIIGFIFPFLIITTSYTLI WKA	217
AT1_Consensus	.α InRNαnFαEN.N.TVα.FμYβ.-N∞TL. αGIGL∞KNαIGFααPFLIILTSYTLI WK.	
AT2_Human	TF YFRDVRTIEYLGVNACIMAFPPPEKYQWS AGIALMKNILGFIIPLIFIAICYFGI RKH	233
AT2_Consensus	TF YFRDVRTIEYLGVNααMAFPPEKYQWS AGIALMKNαLGFIIPLIFIAICYFGI RKH	
MAS_Human	EY -----VMCIDREEESHNRNDC RAWIFIAIISFLVFTPLMLVSSSTIL VVK	208
MAS_Consensus	EY -----αMID...SμS..DC RAWIαFIAαL SFLV...ααVSSSTIL VαK	
Rhodopsin_HUMAN	PL AGWSRYIPEGLQCS-αGIDYYTLKPEVNN ESFVIYMFVVHFTIFMIIFFCVIGQL VFT	229

	HELIX 6	
	614 620 622 627	
AT1_Human	LKKAY----EIQKNKPR NDDIFKIIIMAVLFFFFSKNIHQIFTFIDV LIQLGIIRD CRIA	277
AT1_Consensus	LKμAY----.IQμN..R .DDIFμαIαAIVαFFFFSααPHQαFTFαDV LIQL.αI.DC.I.	
AT2_Human	LLKTN----SYGKNRIT RDQVLKMAAAVVLAFIICNLFFHVLTFIDA LAWMGVINSCEVI	293
AT2_Consensus	LLKTN----SYGKNRIT RDQVLKMAAAVVLAFIICNLFFHVLTFIDA L.WMααINSCEVα	
MAS_Human	IRKNT----WASH--- SSKLYIVIMVTIIIFLIFAMPRLLYLLYY -----EYW	255
MAS_Consensus	IRKNT----W..H--- SSKLYIVI.VTIIαFLIFααPMRαLYLLYY -----EYW	
Rhodopsin_HUMAN	VKEAAAQQQESATTQKA EKEVTRMVIIMVIAFLICNVFYASVAFYIF -----THQGS	281

	HELIX 7	HELIX 8	
	712 719 725 730 734 810		
AT1_Human	DIV DTAMPITICIAFYFNCLNPLF YGFLG KKPKRYFLQLL YIPPKAKSHSNLSTKMSTL		337
AT1_Consensus	DαV DTAMPαTICαAIFYFNCLNPLαF Y.FαG K.FKμRYFLQLαK YIPP.α.∞H..L∞TKMS∞L		
AT2_Human	AVI DLALPFALLLGFNSCVNPFLL YCFVG NRFQKLRVFR VP-----ITWLQGKRESM		347
AT2_Consensus	AVI DLALPFALLLGFNSCVNPFLL YCFVG NRFQKLRVFR VP-----ITWLQGKRE∞M		
MAS_Human	STF GNLHHTISLFFSTINSSANPFI YFFVG SSKKRFKESLK VVL-----TRAFKDEMQPR		310
MAS_Consensus	S.F G.LH.ISLFFSTαNSSANPFI YFFVG SSKKRFβESLK VVL-----TRAFKDEMQPR		
Rhodopsin_HUMAN	NFG PIFMTIPAFFAKSAAIYNEVI YIMMN KQFRNCMLTTIC CG-----KNPLGDDEASA		335

AGTR1_Human	SYRPSDNVSSSTKKPAPCFEVE	359
AT1_Consensus	SYRP.β.....KK.α...β.E	
AT2_Human	SCRKSSSLREMETFVS-----	363
AT2_Consensus	SCRK.SSLREMTβTFVS-----	
MAS_Human	RQKDNCNTVTVETVV-----	325
MAS_Consensus	RQ...NT.∞IETVV-----	
Rhodopsin_HUMAN	TVSKTETSQVAPA-----	348

Figure 4. Sequence alignments of AT1, AT2, MAS, and Rhodopsin from human or the consensus sequence. Consensus sequence alignments show those amino acids conserved as α (A, V, L, I, F, W, M, P), polar acidic as β (D, E), polar basic as μ (K, R, H), aromatic as π (F, W, H, Y), ∞ for S and T conservation, and. for no conservation. Cysteines highlighted in yellow are those identified to form cysteine bridges, amino acids highlighted in red commonly conserved in GPCR, cyan conserved in all sequences including Rhodopsin, green those conserved only in AT1, AT2, and MAS, and gray/magenta those conserved in only AT1 and AT2 that were identified in other experiments to be critical to Ang peptide binding or activation.

doi:10.1371/journal.pone.0065307.g004

magenta). This amino acid when changed in AT1 from an Asn to a Gly leads to an increase activity by the Ang peptide derivative Sar¹, Ile⁴, Ile⁸ that normally provides no activity [33]. This activation is only seen in inositol phosphate signaling and does not result in phosphorylated receptor [34]. This amino acid is believed to interact with Tyr 4 of Ang II. In MAS, a Gly is found at this site (Figure 4), suggesting that Ang peptides may result in differential activation in MAS. Close by this amino acid is a Tyr (Figure 5, magenta, amino acid 723), which likely interacts with amino acid 325. Tyr 4 of Ang II thus likely displaces this interaction. MAS contains a Thr at amino acid 723, further supporting a differential mechanism of activation by MAS.

Mutational results suggest that amino acid 512 (Lys, amino acid 5.42 in the Ballesteros-Weinstein naming scheme) contacts the C-terminus of Ang II, while amino acid 621 (His, 6.51 in the Ballesteros-Weinstein naming scheme) interacts with amino acid 8 (Phe) of Ang II [30]. Both 512 and 621 are conserved in AT1 and AT2, and both are associated with altered phenotype when mutated (Figure 6A–B, blue). However, MAS has an Ile at amino acid 512 and a Met at 621 (Figure 6C). A second conformation of Ang binding to AT1 based on photolabeled experiments shows the C-terminus interacting with an Asn at amino acid 725 [31] (Figure 6A). The structure of AT1, with 512 and 621 identified (Figure 6A, blue), shows aromatic amino acids (Figure 6A, red) that cluster towards amino acid 725. In AT2, however, a Leu at amino acid 336 has been shown to have a photolabeled interaction with the C-terminus [35] (Figure 6B, green). In AT2 there is an additional aromatic amino acid (Phe) close to 336 at amino acid 332 that is not found in AT1 (Leu). This is likely the explanation as to why

AT1 and AT2 have different photolabeled Ang II binding sites. The structure of MAS suggests that the aromatic amino acids would not stabilize the Phe (8) of Ang II (Figure 6C), further suggesting Ang-(1–7) to be the ligand of choice.

Internalization and the pathway of the ligand inside the receptor are more likely to be the main mechanisms of ligand specificity and activation rather than one single binding energy state. Many receptors may contain a site with a high ligand binding rate (static binding), but if the peptides are unable to internalize or unable to transition the receptor into an activated form (dynamic binding), they are biologically inert. AutoDock experiments of both AT1 and MAS for either Ang II or Ang-(1–7), yielded several conformations of high binding energy for the Ang peptides (Figure S6). The top three conformations from each AutoDock experiment were placed onto each of the other receptors and energy minimized (Figure S7). This revealed binding energies for Ang II to be higher on either AT1 or AT2 than that of MAS, while Ang-(1–7) had a similar binding energy to all structures. Visual analysis of the binding of all these experiments shows the Ang peptide to be interacting more extracellular than the mutagenesis data suggests (Figure S8). To combat this, forced docking experiments were performed on AT1 with Ang II's eighth amino acid Phe interacting with 512/621 (Initial binding) or amino acid 725 (Buried binding). The binding energies for both the internalization (based on AutoDock results above) and the initial binding were lower for MAS than AT1 and AT2, suggesting as to why Ang II has a lower binding affinity for MAS (Figure S9A). However, Ang-(1–7) has similar binding energy for MAS compared to AT1 and AT2 (Figure S9B).

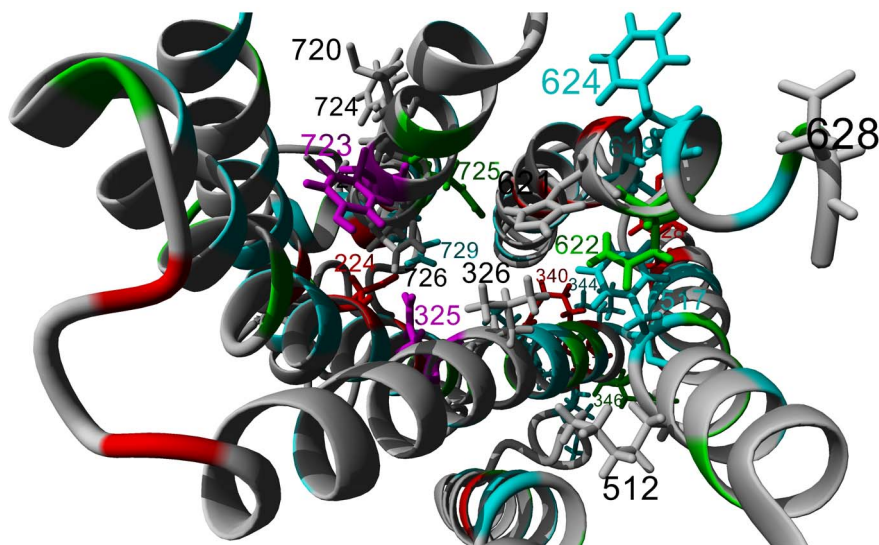


Figure 5. Conservation of amino acids shown on the structure of AT1. View is from looking down the receptor from the extracellular surface. Red indicates amino acids commonly conserved in GPCRs, cyan those conserved with Rhodopsin, and green those conserved only in AT1, AT2 and MAS corresponding to Figure 4. Amino acids shown are those identified in Table S1 to have functional roles in Ang peptides binding and activation of receptors, including the consensus GPCR number used.

doi:10.1371/journal.pone.0065307.g005

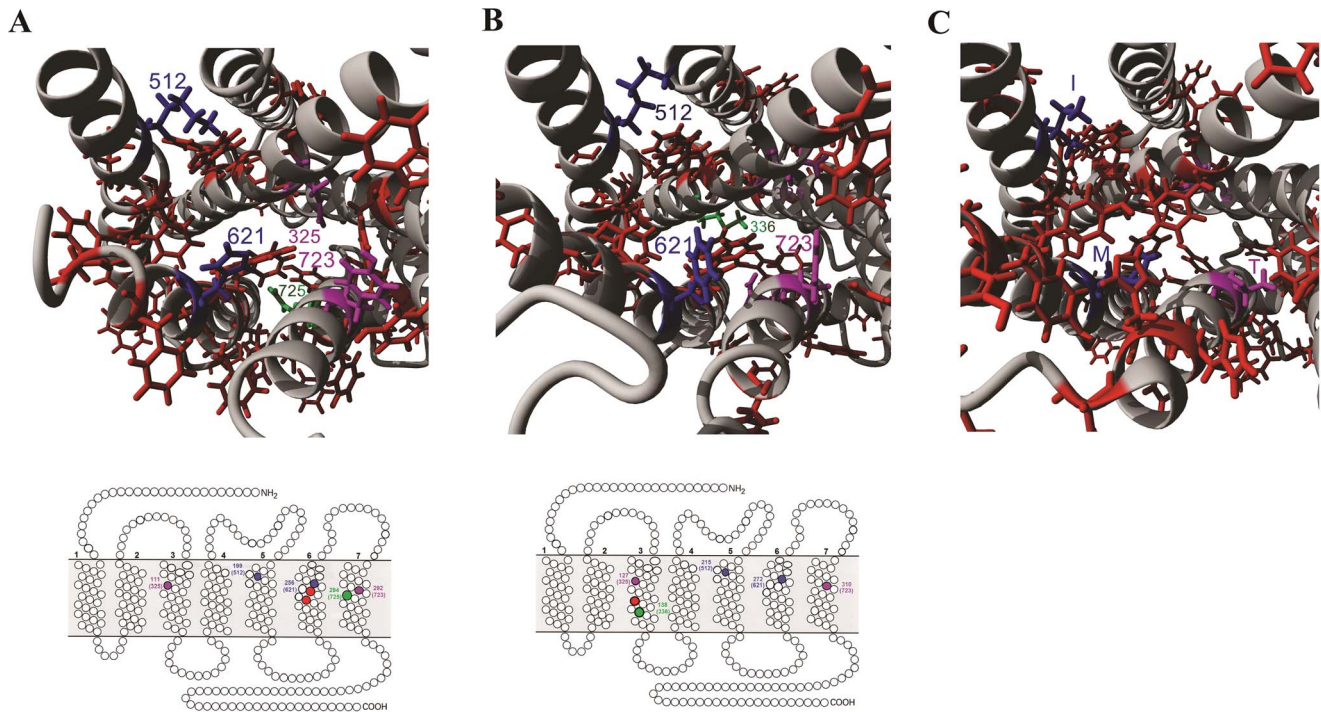


Figure 6. Amino acids involved in activation of AT1 and AT2 but not MAS. Amino acids 512 and 621 (blue) interact with amino acid 8 (Phe) of Ang II, while 325 (magenta) interacts with amino acid 4 (Tyr) of Ang II displacing 723 (Tyr) in both AT1 (A) and AT2 (B). Aromatic amino acids (red) likely serve to transition Phe 8 from 512 and 621 to the known photolabeled interaction sites at 725 for AT1 (A) or 336 for AT2 (B). The basic seven transmembrane domain schematic representation is added below each figure to show the amino acid positions in both AT1 (A) and AT2 (B) with the numbers listed at each site the location in the respective protein, and the number in brackets that used as the common numbering scheme. These mechanisms seen in AT1/AT2 are not conserved in MAS (C).
doi:10.1371/journal.pone.0065307.g006

Molecular dynamics were performed for ten nanoseconds on each of these conformations of AT1. When Ang II was either free from AT1 (Figure 7A, black), interacting with the extracellular loops (Figure 7A, red), or beginning internalization (Figure 7A, green) AT1 had normal carbon alpha RMSDs. When Ang II is bound in the initial binding mode (Figure 7A, magenta) movement started normal, but began increasing around 5 nanoseconds. At this point the movement increased to values seen in the buried binding (Figure 7A, cyan). The stretching of the receptor was observed in the buried binding, and also observed in the initial binding shortly after the simulations started (Figure 7B). The stretching of the receptor can be seen to result in movement of helix 3, a slight rotation of helix 6 and significant movement of helix 5 (Figure 8). Amino acid 8 (Phe) began transitioning towards the buried binding in the initial binding simulation, resulting in the changes starting around 2 nanoseconds.

Discussion

Binding and activation of various GPCRs by Ang peptides likely involves multiple binding modes and conformations of the receptor. Therefore, the activation is not static, but involves a very diverse energy landscape for activation. The binding involves extracellular contacts and internalization, which then complex into initial binding and a buried binding mechanism for activation (Figure 9). Many studies in the past have suggested multiple stages of activation; separating receptor phosphorylation, p42/44 MAPK activation, internalization, and inositol phosphate signaling [33,36–40]. In the case of AT1/AT2 we propose that Ang II

will first complex into an initial binding with Ang II's C-terminus bound to amino acid 512 (Lys) of AT1/AT2, and the side chain of the eighth amino acid (Phe) interacting with the aromatic amino acid 621 (His/Phe) of AT1/AT2. At the same time amino acid 4 (Tyr) of Ang II interacts with amino acid 325 (Asn), displacing amino acid 723, leading to rotation of helix seven. This initial binding likely activates the p42/44 MAPK [37]. This binding is confirmed through mutagenic experiments showing that for receptor activation to occur, amino acid 512 needs to be basic [28] and 621 aromatic [30], while Ang II's eighth amino acid must be aromatic [41].

Photolabeling experiments [31,35] show the final state of peptide/receptor binding, but in the past these data have been thought to be inconsistent with the mutagenic data. We suggest a hypothesis that includes both data sets as valid, where mutagenic data is consistent with inhibition of the initial binding conformation. The ligand is then internalized from the initial binding mode by passing along conserved aromatic residues (614 and 618) through pi-pi interaction to amino acid 725 (Asn) of AT1. In AT2, the additional aromatic amino acid 332 (Phe) causes the Phe (8) of Ang II to move to 336 (Leu). This buried binding conformation likely induces structural conformation changes to the receptor at helices 3, 5, and 6 resulting in inositol phosphate response. This internalization changes Ang II binding from a horizontal-like conformation (in initial binding) to a vertical conformation (in buried), with the pivot point of Ang II at amino acid four (Tyr). In this change, internal packing of AT1 is disrupted, causing expansion of the middle of AT1 and increased movement of amino acids in this region. This expansion exposes amino acids normally not exposed to

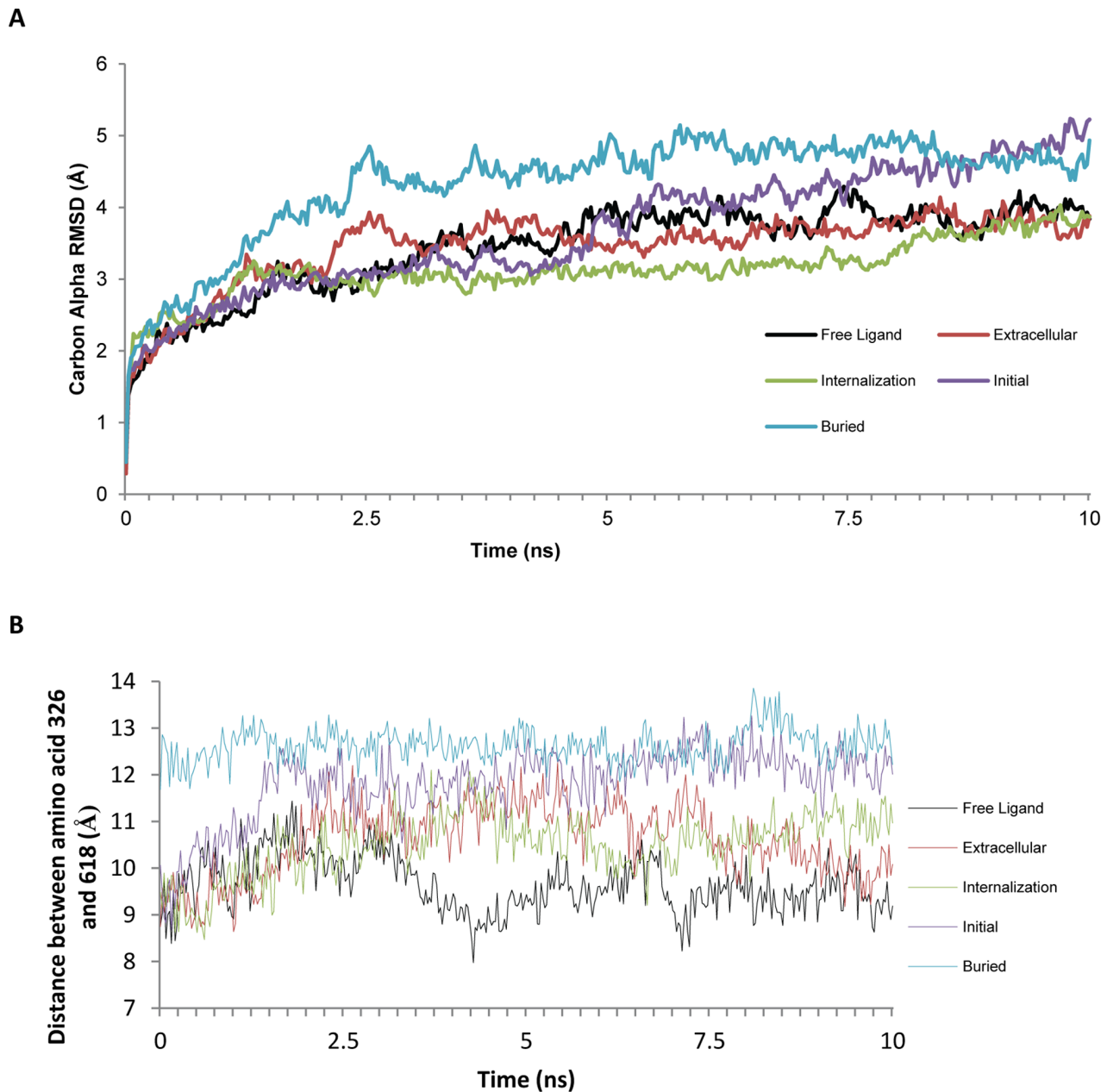


Figure 7. Molecular dynamics simulations of the multiple states of AT1 in activation. The Carbon alpha RMSD of Ang II bound at the multiple points of activation to AT1 (A). The graph shows that the buried position (cyan) yields an increase in overall dynamics of the AT1 receptor. The initial binding (purple) led to a transition in the simulation to yield a similar binding as the buried as the simulation neared 8 ns. **B**) The distance between two of the amino acids (326 and 618) found in the site of AT1 where the eighth amino acid (Phe) comes to the final photolabeled interaction for each of the stages of AT1 activation. This shows that the binding of Ang II in the buried position causes a stretching (around 3 Å), leading to opening of new interaction sites for protein interactions. The initial (purple) binding led to propagation and stretching of the receptor around 2 ns yielding similar values as that of the buried binding.
 doi:10.1371/journal.pone.0065307.g007

the membrane, allowing for recruitment and/or interaction with other membrane proteins. The final position of the Ang binding transition is seen with the photolabeled experiments, while all other states of binding require different tools to visualize that binding state, as they are transitions rather than final configurations.

Amino acid 622, which is adjacent to the aromatic residue 621 in the initial binding conformation, is present as a His in AT2. Mutations of this amino acid are known to affect ligand

binding [42]. AT2 does not have an aromatic amino acid at 724, which is required for interaction with the C-terminus of Ang II in AT1 [31]. This absence (with the addition of Phe 332) likely leads to a different migration from the initial state to the buried state in AT2. Variation in the final buried site alters the dynamics of a separate region of the GPCR, and thus opens a different possible binding site for recruitment of additional proteins. In our models, we also observed very few amino acids conserved between AT1 and AT2 that would likely interact

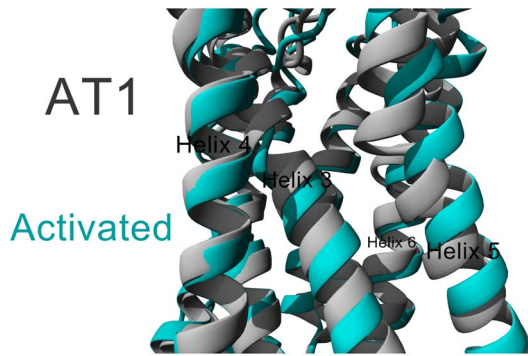


Figure 8. Activated vs. non-activated AT1. The average structure over the 10 ns simulations shown for either AT1 with Ang II free (gray) or in the final buried position (cyan). This shows that Ang II activation likely leads to shifting in helix 3, 5 and 6. This suggests regions of helix 5 (containing the largest movement of the helix) to likely recruit other proteins when Ang II is bound. Additionally some modification made in the intracellular region (due to the shifting of helix 3) could potentially modify intracellular activation.
doi:10.1371/journal.pone.0065307.g008

with the first amino acid of Ang II. Recent evidence suggests that Ang III may be the primary agonist of AT2 in the kidney [43,44]. Our model suggests that no amino acids have been conserved in the sequence divergence between AT1 and AT2 that would interact with amino acid one of Ang II. Amino acid two (Arg) of Ang II has been shown to interact with amino acid 712 (Asp) of AT1 [45] which is conserved in both AT1 and AT2, but not in MAS.

MAS and its related proteins are not activated by Ang II [15]. Our models and sequence analysis reveal that the internalization process differs in MAS compared to AT1 and AT2. Numerous amino acids are conserved in AT1, AT2, and MAS with amino acids 231 (hydrophobic) and 318 (hydropho-

bic) contacting Ang II in our initial binding to MAS. With variations at amino acids 512 and 621 (both hydrophobic in MAS), we suggest an unfavorable interaction with Phe (8) of Ang II, which is removed in Ang-(1-7). Amino acid 325 varies in MAS to amino acids that are known to lead to receptor activation (Gly) in AT1 [33], this suggests that Tyr (4) of Ang-(1-7) may insert into this region inducing structural alterations in helix seven. This alteration likely leads to interactions with other membrane proteins. Several other MAS related proteins have been shown to interact with Ang peptides and activate intracellular pathways. Studying the details of these proteins will allow for the predictions of which proteins interact with MAS to yield activation.

Protein activation of AT1 is likely to be through expansion and rotation of the helices. This is further suggested by mechanical stretch of cells transfected with AT1 leading to activation of intracellular signals without agonist induction [46,47]. These expansions either alter regions on the intracellular side leading to G-protein activation and association with Jak2 through the KYIPP motif [48] or through changing interactions with other membrane bound proteins such as other GPCR [49]. AT1 has been shown to homo-oligomerize [50], or hetero-oligomerize with AT2 [51], Bradykinin B2 receptor [21,52], MAS [53], and CB₁R [54].

In addition to Ang-(1-7), many metabolites of Ang peptides are found. This makes addressing the role of the receptors and other associated proteins such as the angiotensin receptor associated protein (ATRAP) difficult using classical physiology and biochemistry approaches. The use of computational tools expands our current research approach to study possible mechanisms existing for these various components. Having detailed molecular/atomic mechanism provided in this study, allows for new analyses of other Ang peptides such as Ang III and Ang IV, addressing whether they have similar mechanism of activation of AT1 and AT2. Having identified specific amino acids of the receptor that lead to activation by Ang peptides, we

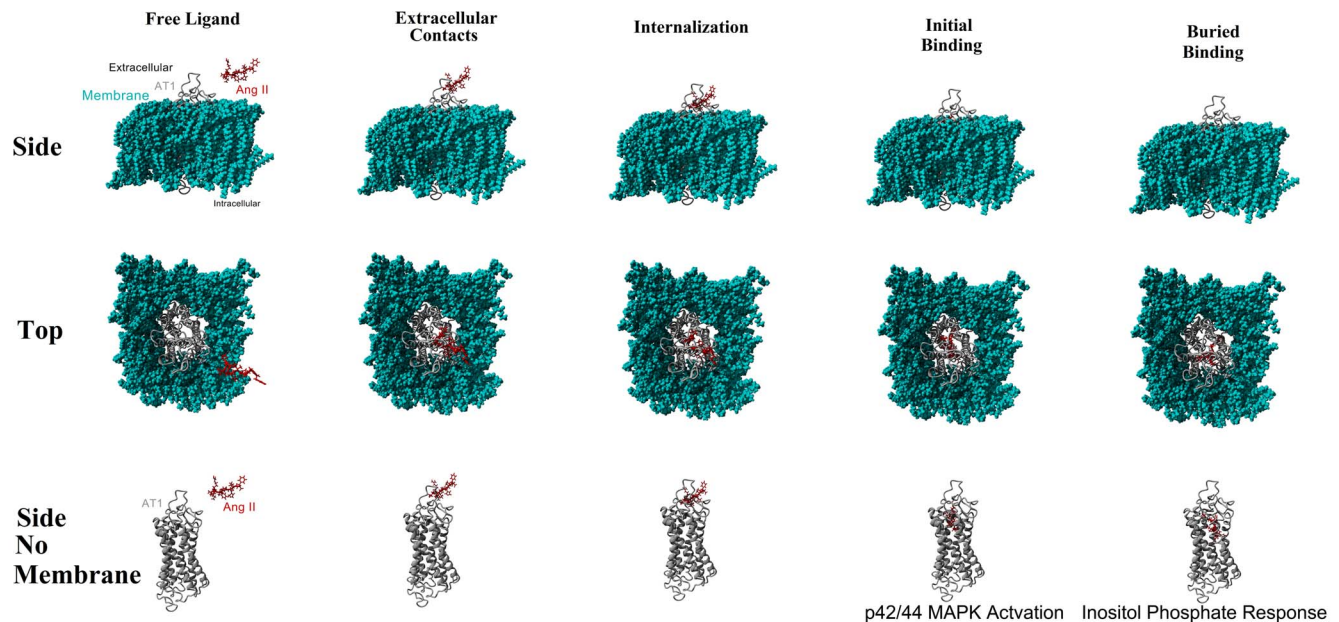


Figure 9. Pathway of activation of AT1 by Ang II. Figure shows the multiple binding states of Ang II activation of AT1 receptor. Initial binding results in movement of helix 7 by Tyr4 of ANG II leading to p42/44 MAPK activation; buried binding results in movement of helix 5 by Phe8 of Ang II leading to Inositol Phosphate response.
doi:10.1371/journal.pone.0065307.g009

can also begin searching other GPCR sequences for other proteins that have the potential to bind and be activated by Ang peptides.

Supporting Information

Figure S1 Dynamics with a disulfide bridge in MAS. A). Location of the two Cys amino acids on the numbering system of MAS. B). Conservation of amino acids in Mouse, Rat and Human. C). Molecular dynamics simulation of our model 1 of MAS (blue) compared to the model with a Cyc-Cys bridge (red) revealing minimal change in the energy or averaged carbon alpha RMSD over a 1 nanosecond simulation.
(TIF)

Figure S2 AT1, AT2 and MAS molecular dynamics simulation data for amino acid carbon alpha RMSDs. Molecular dynamic simulation results showing similar carbon alpha RMSDs for amino acids in the models of AT1, AT2, and MAS in a lipid membrane. The seven transmembrane domains are numbered all showing stability of movement relative to the loops.
(TIF)

Figure S3 AT1 sequence alignments from multiple species. Consensus alignment show amino acids 100% conserved, those conserved as a hydrophobic amino acid as α (A, V, L, I, F, W, M, P), polar acidic as β (D, E), polar basic as μ (K, R, H), aromatic as π (F, W, H, Y), ∞ for S and T conservation, and for no conservation.
(TIF)

Figure S4 AT2 sequence alignments from multiple species. Consensus alignment show amino acids 100% conserved, those conserved as a hydrophobic amino acid as α (A, V, L, I, F, W, M, P), polar acidic as β (D, E), polar basic as μ (K, R, H), aromatic as π (F, W, H, Y), ∞ for S and T conservation, and for no conservation.
(TIF)

Figure S5 Mas sequence alignments from multiple species. Consensus alignment show amino acids 100% conserved, those conserved as a hydrophobic amino acid as α (A, V, L, I, F, W, M, P), polar acidic as β (D, E), polar basic as μ (K, R, H), aromatic as π (F, W, H, Y), ∞ for S and T conservation, and for no conservation.
(TIF)

Figure S6 Top 10 results from the docking ensemble experiment. Yellow bars are those dockings that went on to the top3 macro analysis from each group.
(TIF)

Figure S7 Top three em docking macro results from each of the ten top ligand/receptor docking ensemble

runs (figure S6 in yellow) analyzed on AT1 (blue), AT2 (red), MAS (green), or Rhodopsin (purple).
(TIF)

Figure S8 Structures of the top 3 results of docking (Figure S7) of either AT1 or MAS to either Ang II or Ang-(1-7).
(TIF)

Figure S9 Binding energy of Ang II (A) through either an Autodock experiment representing internalization (blue), the initial binding (red) as identified by forced docking using mutagenesis data, or the buried binding (green) based on photolabeled data. This shows a lower binding energy for MAS at both the internalization and initial thus suggesting why MAS would bind Ang II with a lower affinity than AT1 or AT2. Binding energy for Ang-(1-7) binding however suggests similar energy for all three receptors (B).
(TIF)

Table S1 Amino acids known to have functional roles in AT1, AT2 or MAS with the consensus amino acid # and amino acid found at that location in AT1, AT2, or MAS. A brief description of each is given and the reference for the published role of that amino acid. Some references can be found in the manuscript with additional references listed in the. The amino acid found in each receptor based on sequence alignments is also listed
(XLSX)

Docking_EM_analysis S1 This Macro energy minimizes (EM) the target *in vacuo*, adds water and EM with AMBER 03 force field, then calculates the PE of the receptor/ligand, the BE of the ligand, and the RMSD of initial structure to final structure.
(MCR)

Docking_EM_top3 S1 This Macro analyses the top three results of the docking_EM_analysis macro and compares them to the structure when complexed and EM to AT1, MAS, AT2, and Rhodopsin.
(MCR)

Additional References S1 Material referenced in Table S1
(DOCX)

Acknowledgments

We would like to acknowledge Dr. Robert Carey for his advice and review of material for clinical relevance and impact.

Author Contributions

Conceived and designed the experiments: JWP RASS AM. Performed the experiments: JWP. Analyzed the data: JWP RASS AM. Contributed reagents/materials/analysis tools: JWP RASS AM. Wrote the paper: JWP.

References

- DeMello WC, Frohlich ED (2010) Renin angiotensin system and cardiovascular disease. New York: Humana Press. 300p.
- Zhou A, Carrell RW, Murphy MP, Wei Z, Yan Y, et al. (2010) A redox switch in angiotensinogen modulates angiotensin release. *Nature* 468: 108–111.
- Morales R, Watier Y, Boxskai Z (2012) Human prorenin structure sheds light on a novel mechanism of its autoinhibition and on its non-proteolytic activation by the (pro)renin receptor. *J Mol Biol* 421: 100–111.
- Danser JAH, Batenburg WW, van Esch JH (2007) Prorenin and the (pro)renin receptor—an update. *Nephrol Dial Transplant* 22: 1288–1292.
- Santos RA, Ferreira AJ, Simoes E Silva AC (2008) Recent advances in the angiotensin-converting enzyme 2-angiotensin(1-7)-Mas axis. *Exp Physiol* 93: 519–527.
- Zini S, Fournic-Zaluski MC, Chauvel E, Roques BP, Corvol P, et al. (1996) Identification of metabolic pathways of brain angiotensin II and III using specific aminopeptidase inhibitors: predominant role of angiotensin III in the control of vasopressin release. *Proc Natl Acad Sci U S A* 93: 11968–11973.
- Murphy TJ, Alexander RW, Griendling KK, Runge MS, Bernstein KE (1991) Isolation of a cDNA encoding the vascular type-1 angiotensin II receptor. *Nature* 351: 233–236.
- Steckelings UM, Paulis L, Namsolleck P, Unger T (2012) AT2 receptor agonists: hypertension and beyond. *Curr Opin Nephrol Hypertens* 21: 142–146.
- Ito M, Oliverio MI, Mannon PJ, Best CF, Maeda N, et al. (1995) Regulation of blood pressure by the type 1A angiotensin II receptor gene. *Proc Natl Acad Sci U S A* 92: 3521–3525.

10. Schorb W, Booz GW, Dostal DE, Conrad KM, Chang KC, et al. (1993) Angiotensin II is mitogenic in neonatal rat cardiac fibroblasts. *Circ Res* 72: 1245–1254.
11. Ichiki T, Labosky PA, Shiota C, Okuyama S, Imagawa Y, et al. (1995) Effects on blood pressure and exploratory behavior of mice lacking angiotensin II type-2 receptor. *Nature*. 377: 748–750.
12. Stoll M, Steckelings UM, Paul M, Bottari SP, Metzger R, et al. (1995) The angiotensin AT2-receptor mediates inhibition of cell proliferation in coronary endothelial cells. *J Clin Invest* 95: 651–657.
13. Jackson TR, Blair LA, Marshall J, Goedert M, Hanley MR (1988) The mas oncogene encodes an angiotensin receptor. *Nature* 335: 437–440.
14. Santos RA, Simoes e Silva AC, Maric C, Silva DM, et al. (2003) Angiotensin-(1–7) is an endogenous ligand for the G protein-coupled receptor Mas. *Proc Natl Acad Sci U S A* 100: 8258–8263.
15. Gembardt F, Grajewski S, Vahl M, Schultheiss HP, Walther T (2008) Angiotensin metabolites can stimulate receptors of the Mas-related genes family. *Mol Cell Biochem* 319: 115–123.
16. Underwood DJ, Strader CD, Rivero R, Patchett AA, Greenlee W, et al. (1994) Structural model of antagonist and agonist binding to the angiotensin II, AT1 subtype, G protein coupled receptor. *Chem Biol* 1: 211–221.
17. Balcanu-Gogonea C, Karnik S (2006) Model of the whole rat AT1 receptor and the ligand-binding site. *J Mol Model* 12: 325–337.
18. Oliveira L, Costa-Neto CM, Nakaie CR, Schreiber S, Shimuta SI, et al. (2007) The Angiotensin II AT1 Receptor Structure-Activity Correlations in the Light of Rhodopsin Structure. *Physiol Rev* 87: 565–592.
19. Nikiforovich GV, Marshall GR (2001) 3D model for TM region of the AT-1 receptor in complex with angiotensin II independently validated by site-directed mutagenesis data. *Biochem Biophys Res Commun* 286: 1204–1211.
20. Sköld C, Nikiforovich G, Karlén A (2008) Modeling binding modes of angiotensin II and pseudopeptide analogues to the AT2 receptor. *J Mol Graph Model* 26: 991–1003.
21. AbdAlla S, Lother H, Quitterer U (2000) AT1-receptor heterodimers show enhanced G-protein activation and altered receptor sequestration. *Nature* 407: 94–98.
22. Prinster SC, Hague C, Hall RA (2005) Heterodimerization of G protein-coupled receptors: specificity and functional significance. *Pharmacol Rev* 57: 289–298.
23. Zhang Y (2008). I-TASSER server for protein 3D structure prediction. *BMC Bioinformatics* 9: 40.
24. Roy A, Kucukural A, Zhang Y (2010) I-TASSER: a unified platform for automated protein structure and function prediction. *Nat Protocols* 5: 725–738.
25. Duan Y, Wu C, Chowdhury S, Lee MC, Xiong G, et al. (2003) A point-charge force field for molecular mechanics simulations of proteins based on condensed-phase quantum mechanical calculations. *J Comput Chem* 24: 1999–2012.
26. Konagurthu AS, Whisstock JC, Stuckey PJ, Lesk AM (2006) MUSTANG: A multiple structural alignment algorithm. *Proteins* 64: 559–574.
27. Spyroulias GA, Nikolakopoulou P, Tzakos A, Gerotheranassis IP, Magafa V, et al. (2003) Comparison of the solution structures of angiotensin I & II. Implication for structure-function relationship. *Eur J Biochem* 270: 2163–2173.
28. Yamano Y, Ohyama K, Chaki S, Guo DF, Inagami T (1992) Identification of amino acid residues of rat angiotensin II receptor for ligand binding by site directed mutagenesis. *Biochem Biophys Res Commun* 187: 1426–1431.
29. Pulakat L, Tadesse AS, Dittus JJ, Gavini N (1998) Role of Lys215 located in the fifth transmembrane domain of the AT2 receptor in ligand-receptor interaction. *Regul Pept* 73: 51–57.
30. Noda K, Saad Y, Karnik SS (1995) Interaction of Phe8 of angiotensin II with Lys199 and His256 of AT1 receptor in agonist activation. *J Biol Chem* 270: 28511–28514.
31. Pérodin J, Deraet M, Auger-Messier M, Boucard AA, Rihakova L, et al. (2002) Residues 293 and 294 are ligand contact points of the human angiotensin type 1 receptor. *Biochemistry* 41: 14348–14356.
32. Zhang Y, Devries ME, Skolnick J (2006) Structure modeling of all identified G protein-coupled receptors in the human genome. *PLoS Comput Biol* 2: e13.
33. Noda K, Feng YH, Liu XP, Saad Y, Husain A, et al. (1996) The active state of the AT1 angiotensin receptor is generated by angiotensin II induction. *Biochemistry* 35: 16435–16442.
34. Thomas WG, Qian H, Chang CS, Karnik S (2000) Agonist-induced phosphorylation of the angiotensin II (AT1A) receptor requires generation of a conformation that is distinct from the inositol phosphate-signaling state. *J Biol Chem* 275: 2893–2900.
35. Servant G, Laporte SA, Leduc R, Escher E, Guillemette G (1997) Identification of angiotensin II-binding domains in the rat AT2 receptor with photolabeled angiotensin analogs. *J Biol Chem* 272: 8653–8659.
36. Hunyady L, Vauquelin G, Vanderheyden P (2003) Agonist induction and conformational selection during activation of a G-protein-coupled receptor. *Trends Pharmacol Sci* 24: 81–86.
37. Hines J, Fluharty SJ, Yee DK (2003) Structural determinants for the activation mechanism of the angiotensin II type 1 receptor differ for phosphoinositide hydrolysis and mitogen-activated protein kinase pathways. *Biochem Pharmacol* 66: 251–262.
38. Holloway AC, Qian H, Pipolo L, Ziogas J, Miura S, et al. (2002) Side-chain substitutions within angiotensin II reveal different requirements for signaling, internalization, and phosphorylation of type 1A angiotensin receptors. *Mol Pharmacol* 61: 768–777.
39. Vauquelin G, Van Liefde I (2005) G protein-coupled receptors: a count of 1001 conformations. *Fundam Clin Pharmacol* 19: 45–56.
40. Kobilka BK, Deupi X (2007) Conformational complexity of G-protein-coupled receptors. *Trends Pharmacol Sci* 28: 397–406.
41. Aumelas A, Sakarellos C, Lintner K, Fermanjian S, Khosla MC, et al. (1985) Studies on angiotensin II and analogs: impact of substitution in position 8 on conformation and activity. *Proc Natl Acad Sci U S A* 82: 1881–1885.
42. Turner CA, Cooper S, Pulakat L (1999) Role of the His273 located in the sixth transmembrane domain of the angiotensin II receptor subtype AT2 in ligand-receptor interaction. *Biochem Biophys Res Commun* 257: 704–707.
43. Kemp BA, Bell JF, Rottkamp DM, Howell NL, Shao W, et al. (2012) Intrarenal angiotensin III is the predominant agonist for proximal tubule angiotensin type 2 receptors. *Hypertension* 60: 387–395.
44. Padia SH, Carey RM (2013) AT2 receptors: beneficial counter-regulatory role in cardiovascular and renal function. *PLoS Arch* 465: 99–110.
45. Feng YH, Noda K, Saad Y, Liu XP, Husain A, et al. (1995) The Docking of Arg of Angiotensin II with Asp of AT Receptor Is Essential for Full Agonism. *J Biol Chem* 270: 12846–12850.
46. Yasuda N, Akazawa H, Qin Y, Zou Y, Komuro I (2008) A novel mechanism of mechanical stress-induced angiotensin II type 1-receptor activation without the involvement of angiotensin II. *Naunyn-Schmiedeberg Arch Pharmacol* 377: 393–399.
47. Yasuda N, Miura S, Akazawa H, Tanaka T, Qin Y, et al. (2008) Conformational switch of angiotensin II type 1 receptor underlying mechanical stress-induced activation. *EMBO Rep* 9: 179–186.
48. Ali MS, Sayeski PP, Dirksen LB, Hayzer DJ, Marrero MB, et al. (1997) Dependence on the motif YIPP for the physical association of Jak2 kinase with the intracellular carboxyl tail of the angiotensin II AT1 receptor. *J Biol Chem* 272: 23382–23388.
49. Ferre S, Franco R (2010) Oligomerization of G protein-coupled receptors: A reality. *Curr Opin Pharmacol* 10: 1–5.
50. Szalai B, Barkai L, Turu G, Szidonya L, Varnai P, et al. (2012) Allosteric interactions within the AT1 angiotensin receptor homodimer: role of the conserved DRY motif. *Biochem Pharmacol* 84: 477–485.
51. AbdAlla S, Lother H, Abdel-tawab AM, Quitterer U (2001) The Angiotensin II AT2 Receptor Is an AT1 Receptor Antagonist. *J Biol Chem* 276: 39721–39726.
52. AbdAlla S, Lother H, el Massiery A, Quitterer U (2001) Increased AT1 receptor heterodimers in preeclampsia mediate enhanced angiotensin II responsiveness. *Nat Med* 7: 1003–1009.
53. Kostenis E, Milligan G, Christopoulos A, Sanchez-Ferrer CF, Heringer-Walther S, et al. (2005) G-Protein-Coupled Receptor Mas Is a Physiological Antagonist of the Angiotensin II Type 1 Receptor. *Circulation* 111: 1806–1813.
54. Rozenfeld R, Gupta A, Gagnidze K, Lim MP, Gomes I, et al. (2011) AT1R-CB1R heteromerization reveals a new mechanism for the pathogenic properties of angiotensin II. *EMBO* 30: 2350–2363.